GeoResJ 5 (2015) 47–56

Contents lists available at ScienceDirect

GeoResJ

journal homepage: www.elsevier.com/locate/GRJ

Temperatures, thermal structure, and behavior of eruptions at Kilauea and Erta Ale volcanoes using a consumer digital camcorder

Gregory T. Carling [a], Jani Radebaugh [a,*], Takeshi Saito [b], Ralph D. Lorenz [c], Anne Dangerfield [d,1], David G. Tingey [a], Jeffrey D. Keith [a], John V. South [e,2], Rosaly M. Lopes [f], Serina Diniega [f]

[a] Department of Geological Sciences, Brigham Young University, S-389 ESC, Provo, UT 84602, USA
[b] Department of Geology, Faculty of Science, Shinshu University, Asahi 3-1-1, Matsumoto 390-8621, Japan
[c] Johns Hopkins University, Applied Physics Laboratory, Laurel, MD 20723, USA
[d] Exxon Mobile Corporation, 745 Highway 6, S. Houston, TX 77079, USA
[e] Wexpro Company, Salt Lake City, UT 84111, USA
[f] Jet Propulsion Laboratory, California Institute of Technology, Pasadena, CA 91109, USA

ARTICLE INFO

Article history:
Received 8 July 2014
Revised 29 December 2014
Accepted 2 January 2015
Available online 28 January 2015

Keywords:
Remote sensing
Volcanism
Kilauea
Erta Ale
Thermal camera
Camcorder

ABSTRACT

Remote thermal monitoring of active volcanoes has many important applications for terrestrial and planetary volcanic systems. In this study, we describe observations of active eruptions on Kilauea and Erta Ale volcanoes using a short-wavelength, high-resolution, consumer digital camcorder and other non-imaging thermal detectors. These systems revealed brightness temperatures close to the eruption temperatures and temperature distributions, morphologies and thermal structures of flow features, tube systems and lava fountains. Lava flows observed by the camcorder through a skylight on Kilauea had a peak in maximum brightness temperatures at 1230 °C and showed brightness temperature distributions consistent with most rapid flow at the center. Surface brightness temperatures of cooling lava flows on Kilauea were close to 850 °C. Centimeter-scale thermal features are evident around pahoehoe ropes and inflated flows and stalactites in lava tubes. Observations of the fountaining Erta Ale lava lake in February 2011 extend the baseline of observations of the eruptive episode begun in late 2010. We observed a fountain using the camcorder and found a peak in maximum brightness temperatures at 1164 °C, consistent with previous studies. Steep temperature gradients were observed across centimeter-scale distances between the highly exposed fountain and cracks and the much cooler lava lake surface and crater walls. The instrument and methods described here lead to robust pictures of the temperatures and temperature distributions at these volcanoes and reveal desired characteristics of planetary remote sensing platforms for the study of volcanically active bodies such as Io.

1. Introduction

Given the increase in variety and availability of aerial, orbiting, and handheld remote sensing instruments, monitoring of active volcanoes from a distance has become widespread [1–4]. Remote thermal monitoring of active volcanoes is important for safely estimating eruption temperatures, determining eruption characteristics such as lava effusion rates, lava composition and eruption style, and validating lava flow models [3,5–12]. Remote sensing methods also have implications for planetary science because this is the only way to obtain data from, for example, active volcanoes on Jupiter's moon Io [13–15]. With improvements in camera technology, thermal monitoring of active volcanoes is becoming more accessible in terms of financial cost and array of available instrument types.

Handheld thermal cameras, in particular, have advanced technologically in recent years and have yielded important results for thermal and behavioral studies of volcanic eruptions [5,16]. These cameras make use of an array of pixels to generate a thermal image and are widely used to measure eruption temperatures, estimate lava volume and heat fluxes, and track morphological changes

* Corresponding author. Tel.: +1 801 422 9127; fax: +1 801 422 0267.
E-mail addresses: greg.carling@byu.edu (G.T. Carling), janirad@byu.edu (J. Radebaugh), saito@shinshu-u.ac.jp (T. Saito), ralph.lorenz@jhuapl.edu (R.D. Lorenz), anne.dangerfield@exxonmobil.com (A. Dangerfield), david_tingey@byu.edu (D.G. Tingey), jeff_keith@byu.edu (J.D. Keith), johnvsouth@gmail.com (J.V. South), rosaly.m.lopes-gautier@jpl.nasa.gov (R.M. Lopes), Serina.Diniega@jpl.nasa.gov (S. Diniega).
[1] Present address.
[2] Present address.

http://dx.doi.org/10.1016/j.grj.2015.01.001
2214-2428/

during an eruption e.g., [4,5,16–26]. Thermal cameras are rapidly increasing in spatial resolution and temperature range. For example, the Forward Looking Infrared (FLIR) T640 has 640 × 480 pixels and a peak temperature of 2000 °C though at a fairly high cost (US $27,950).

Consumer-grade cameras can also be used for remote thermal monitoring of active volcanoes, with many advantages over traditional thermal cameras. For example, Saito et al. [27] developed a technique of radiation thermometry using a low-cost Sony Handycam (US $1000) as a thermal camera in the sub-micron wavelength band. The charge-coupled device (CCD) in the Handycam detects a spectral range from the visible through near-infrared (~0.3–1.0 μm). This style of thermal imaging has the primary benefits of (1) superior image resolution to most other thermal cameras and (2) short wavelength data collection, which enables measurement of actual lava eruption temperatures. There is the added benefit that radiation at 1 μm suffers less absorption by volcanic gases, especially SO_2, than at longer wavelengths [5]. Using the digital camcorder, Saito et al. [27] measured pixel-integrated temperatures as high as 800 °C at Aso volcano, Japan, which more closely approached eruption temperatures relative to previous measurements on the volcano using infrared thermometers.

We utilize this accessible, high-resolution, short-wavelength and low-cost data collection system, along with another low-cost thermal infrared data system, to characterize the eruption at a lava flow and tube flow at Kilauea volcano, Hawaii in 2006 and a fountaining lava lake on Erta Ale in 2011. Our studies reveal the eruption temperatures, temperature distributions and fine-scale morphologies of lavas in these distinct scenarios. We demonstrate that the camcorder provides viable results for high-temperature lavas (>1100 °C) and we describe details of the tube and surface flows on Kilauea. We also describe the lava lake behavior at Erta Ale, extending the temporal baseline for other recent observations of the eruption at this remote volcano.

2. Methods

2.1. Field campaigns

During February 2006, we characterized lava temperatures and lava thermal morphologies at a single tube-fed flow system on the plains south of the Pu'u 'O'o source on Kilauea volcano, Hawaii, using a variety of remote and contact measurements (Fig. 1). We used a Sony Handycam HDR-HC1 to photograph a skylight and two surface breakout flows: one at close range (<5 m) and the other at long range (~2 km) (Fig. 1). At the skylight, core, roof, and wall temperatures were also measured in-situ using a K-type thermocouple and remotely using an optical pyrometer (Omega Omegascope OS3750). At the close-range surface breakout flow, temperatures were measured in-situ with the thermocouple.

During February 2011, we observed the lava lake at Erta Ale volcano, Afar Rift, Ethiopia using the Sony Handycam HDR-HC1 (Fig. 2). The lake was observed entirely at night. Our observations followed just two months after a significant field campaign by [28], which will be discussed subsequently in detail. Video of the lake during our February 2011 campaign can be seen here: (http://youtu.be/XlDJJoFtXIA). We also obtained data of the lava lake eruption using four nonimaging detectors in a side-by-side array (Table 1).

2.2. Obtaining thermal images from the camcorder

The Sony Handycam HDR-HC1 camcorder operates in Normal mode, which records visible wavelengths (0.3–0.8 μm), and NightShot mode, which records visible through near-infrared wavelengths (0.3–1.0 μm). The radiant energy from volcanic features is recorded as individual pixel brightness values that are converted to temperatures. Materials (basalts, in this case) are heated in an oven to 1000 °C and allowed to cool while being monitored by the camera and a thermocouple to develop correlations between pixel brightness and temperature [27]. This relationship has been encoded into the specially created Thermoshot software, which also includes variables such as gain, shutter speed ([27]; http://www.gaia.h.kyoto-u.ac.jp/~thermoshot/index_e.htm) and now aperture value. Thus, images obtained in a variety of conditions can be converted to temperature maps.

The Thermoshot software converts grayscale bitmap images into thermal images based on corrected pixel brightness (I_c):

$$I_c = \frac{I_m^{\gamma} S}{10^{G/20}} \times \left(\frac{F}{F_0}\right)^2 \quad (1)$$

where I_m is the measured brightness taken from a scale of 1 to 256 for grayscale images, γ is the gamma value 2.2 for the NTSC standard, S is camcorder shutter speed, G is gain, F is the aperture value for that image and F_0 is the maximum aperture value (1.8 for this model). The software converts I_c to brightness temperature for each pixel based on the calibration curve shown in Fig. 3. Aperture value was not originally included because in NightShot mode this value is fixed at 1.8, which is the mode in which Saito et al. [27] collected their data. For all images in this study, the aperture value remained 1.8 and this correction was not needed.

Thermoshot was created using a Sony Handycam DCR-PC120, but we obtained the newer Sony Handycam HDR-HC1 because it has high definition video capabilities (DCR-PC120 does not) and it produces higher-resolution images (2.8 megapixels, 1920 × 1440 CMOS sensor, as opposed to 1.6 megapixels for DCR-PC120). Even newer Sony Handycam HDR models are smaller and have up to 34 megapixel resolution. We undertook a calibration of the HDR-HC1 using similar methods to that of Saito et al. (2005), cooling of a heated rock in an oven monitored with a thermocouple, in both Normal and NightShot modes. Fig. 3 compares the I_c-temperature relationship calibration curves for the two camcorders. In Normal mode, there was a difference of <5% between the two camcorders at temperatures >600 °C and a difference of 5–10% at temperatures <600 °C. In NightShot mode, differences ranged from 3% to 14% between the two camcorders, with the HDR-HC1 showing higher I_c at any given temperature relative to DCR-PC120 (Fig. 3).

Note that the calibration curves for both cameras produced by observing a cooling rock have an upper limit of 900 °C for Normal mode and 600 °C for NightShot mode, as a result of experimental limitations and the thermal response of the material at different wavelengths (the higher-temperature, shorter-wavelength component is overwhelmed by the near-infrared response in NightShot mode). However, the curve that fits these data can be extrapolated to higher temperatures, and this is encoded into the Thermoshot software. Several measurements obtained of a soldering iron at temperatures above 1000 °C matched the calibration curve fit, giving confidence in the camera's response at high temperatures. In addition, images of exposed lava obtained in the field and converted to temperature maps with the Thermoshot software produced temperatures that were within 100 °C of concurrent pyrometer measurements (see Section 3.1).

3. Field observations of temperatures and eruption styles

3.1. Kilauea skylights

During February 2006, we characterized lava temperatures and the distribution of temperatures inside a skylight at Kilauea,

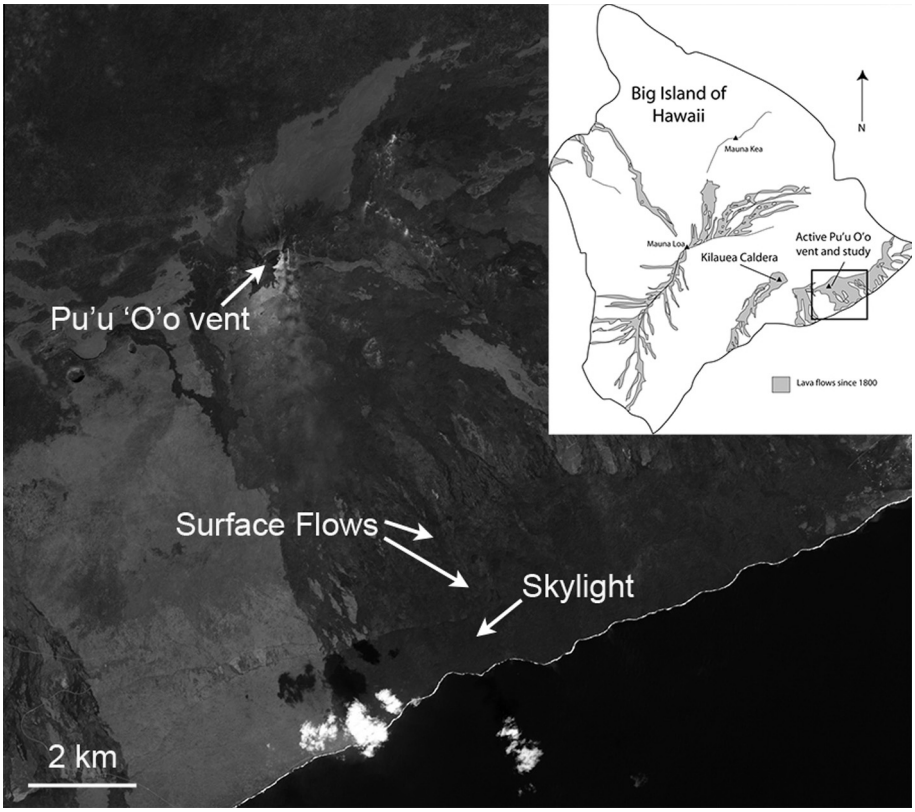

Fig. 1. Study area on Kilauea volcano, Hawaii (inset) in Feb. 2006. The surface flows were observed from near the lower "Surface Flows" arrowhead (the upper "Surface Flows" arrowhead indicating the flows observed from a distance) and the skylight was observed from two locations in very close proximity to each other near the "Skylight" arrowhead. All Kilauea lavas in this study were part of the same tube-contained flow with occasional breakouts. Image from the Advanced Land Imager (ALI), acquired Oct. 29, 2011, courtesy of NASA.

Hawaii (Fig. 4). Images were collected from two different viewpoints at the skylight (Fig. 4a–d) using the Normal mode of the Sony Handycam HDR-HC1 from a distance of ~5 m from the skylight opening. The digital images of the skylight (Fig. 4a and c) reveal a concentration of hot, exposed lava in the center of the opening. The corresponding thermal images (right side of Fig. 4) produced by the Thermoshot software have an assigned color scale (reassigned for each image, to show the full brightness temperature distribution in each scene). White, red and yellow represent the highest brightness temperatures, green and blue are cooler, and dark blue to black represent ambient brightness temperatures.

A peak in the maximum brightness temperature distribution is found at 1230 °C for the hottest material in the open channel of the lava stream in the skylight, with some pixels reaching 1272 °C (Fig. 4b). The visco-elastic skin on the surface of the open channel is ~1100–1200 °C and temperatures in the walls and roof of the skylight range from 750 to 1100 °C. Brightness temperatures on the edge of the skylight are <600°–750 °C.

The viewing angle into the skylight had some effect on the obtained pixel brightnesses and resultant brightness temperatures. This has been noted to be important on Earth [29,21] and on Jupiter's moon Io [30]. Observations into the same skylight from a different viewing angle (Fig. 4d) show temperatures of 1208 °C for the hottest material in the open channel. These values are below those shown in Fig. 4b, perhaps because in Fig. 4b the lava is more directly exposed in the channel center where flow velocities are highest, precluding formation of a skin (see Section 3.5). Temperatures in the skylight walls and roof range from 750 to 1100 °C, and temperatures on the edge of the skylight are <600 °C–750 °C, similar to the values shown in Fig. 4b.

The skylight in Fig. 4a and c was also observed with an Omegascope OS3750 optical pyrometer. The pyrometer has a 0.5° field of view for measurements of ~1–1.2 cm spots and operates in the 0.9 and 1.55 μm wavelengths with a temperature range of 600–2000 °C and an accuracy rating of ±0.6% between 1000 and 1500 °C (Table 1). Maximum measured temperatures of 1165 °C were obtained with this instrument. Our measured values obtained with the camcorder were above those obtained with the pyrometer, perhaps because the high resolution of our camcorder images allowed for imaging only exposed hot material. However, it is also possible the camcorder overestimated temperatures, based on comparison with the pyrometer value and with previous determinations of temperatures.

Previous measurements of temperatures at skylights and channels at Kilauea yielded similar temperatures to within 100 °C. Temperatures of 1165 °C were measured previously using an optical pyrometer [31]. Pinkerton et al. [32] used systematic hand-held radiometer measurements to estimate four thermal components of surface flows: core (>1050 °C); visco-elastic skin (750–900 °C); rigid solid crust (<750 °C); and flow margins (<175 °C). Flynn and Mouginis-Mark [2] determined temperatures in a lava channel using a spectroradiometer and estimated temperatures of 940 °C for the crust and 1120 °C for the hot component. Witter and Harris [24] used a FLIR camera to measure temperatures of 1017–1132 °C for lava surfaces and 1161 °C for the lava core in an active tube.

3.2. Kilauea surface flows

In February 2006, we used the Sony Handycam HDR-HC1 camcorder to photograph two surface breakout flows—one at long range (~2 km) and the other at close range (~10 m) (Fig. 1). The long-range surface breakout flow was photographed at night using the Normal mode, and the close-range surface breakout flow was photographed on an overcast day using NightShot mode and an

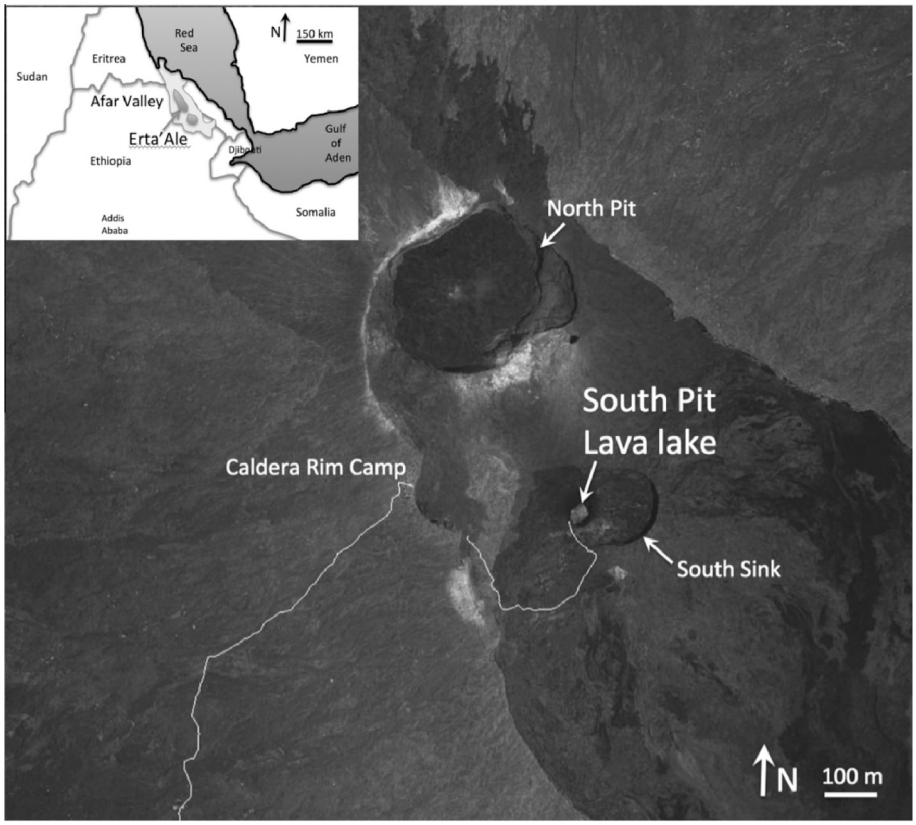

Fig. 2. Location map of the Erta Ale volcano, contained within the Afar Valley, Ethiopia (inset). The lava lake sits within the South Pit, in the South Sink, in the main caldera at the summit of the basaltic shield volcano. Our hiking route is indicated by the white GPS track. We viewed the lava lake from the end of the GPS track on the southwestern edge of the South Pit crater. Image courtesy of Google Earth.

Table 1
Instrumental characteristics

Sony HDR-HC1		Omegascope OS3750	Nonimaging detectors
Sensor	5.9 mm (1/3 type) CMOS	InGaAs and Si	CdS photocell Si LED InGaAs photodiode, thermopile
Pixels	2.969 MegaPixels	640 × 480	–
Lens	Carl Zeiss Vario-Sonnar T	20 mm diameter	–
Focal length	5.1 mm–51 mm	–	–
Filter diameter	37 mm	–	–
Wavelength 1	0.3–0.8 μm visible	0.9 μm	0.94 μm
Wavelength 2	0.3–1.0 μm NightShot	1.55 μm	1.3 μm
T range	~300–1200 °C	600–2000 °C	0–180 °C
Temporal range	~1/s	~1/5 s	5/s

IR-85 longpass filter to exclude solar reflection from the lava radiation signal. Fig. 4e is an image of the surface flow photographed using the Normal mode from a distance of ~2 km. Maximum brightness temperatures of 850 °C were measured for the hottest parts of the surface flow. These maximum temperatures are lower than those for exposed lava in skylights because of the effects of rapidly cooling flow surfaces, atmospheric attenuation and pixel integration as a result of greater viewing distance [29,33]. A future study should include more thorough analysis of the effects of long distance on the camcorder; however, these images show the effectiveness of the camcorder in obtaining temperatures and distributions of temperatures at relatively great distances for field observations.

Fig. 4g is an image of the surface flow that was observed at close range in daytime using the NightShot mode and an IR-85 longpass filter. The effect of solar radiation was minimized because of the filter and because the images were collected on an overcast day; therefore, most high-temperature features are thermal and not reflected energy. Maximum brightness temperatures of 845 °C were measured in the hottest parts of the flow, which occurred in the front of the flow lobes. In contrast, brightness temperatures up to 1120 °C were measured via thermocouple. Higher brightness temperatures were likely not recorded with the HDR-HC1 camcorder for several reasons. Exposed lava corresponds to the white in Fig. 4g and represents a small fraction of the overall flow, because surface flows quickly become insulated by a cooling crust. These flows lose heat faster and thus are cooler overall than lava streams contained in insulated tubes e.g., [34,24]. In addition, using NightShot mode and the longpass filter restricted the short-wavelength portion of the thermal radiance, even in the exposed lavas, making it more difficult to obtain the high-temperature component of the radiance. The exercise of

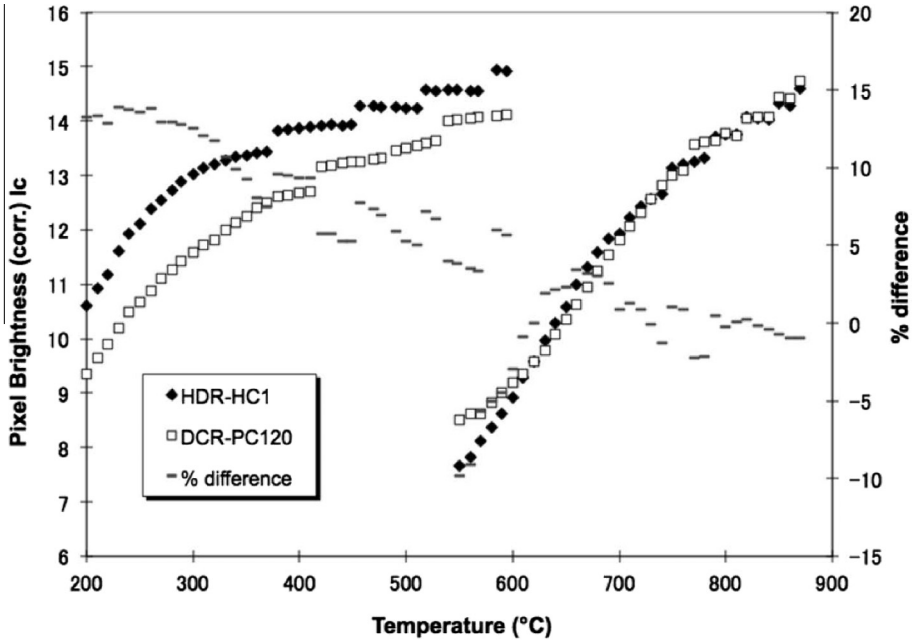

Fig. 3. Relationship between temperature and corrected brightness (*Ic*) in the normal mode (diamonds) and NightShot mode (squares). Camcorder pixel brightness is on the *y*-axis, thermocouple temperature is on the *x*-axis. The percent difference scale on the right *y*-axis reveals a close correlation between the cameras in normal mode and a several percent difference between them in NightShot mode.

observing the surface flow in daytime, using NightShot mode, was thus more valuable for obtaining relative temperature distribution and morphology (see Section 3.5) than for obtaining exposed lava temperatures.

3.3. Erta Ale lava lake

We observed the lava lake contained within the summit caldera of the Erta Ale basaltic shield volcano in February 2011 at night. Our observations happened two months after a major eruptive episode observed by a ground team in November–December 2010 [28]. During their observations, the lava lake filled the South Pit crater, which typically contains the lava lake, and lavas flowed onto the floor and overtopped the western margin of the larger South Sink crater. This led to emplacement of lava flows on the caldera floor that extended to the western caldera rim (termed "main crater" rim by Field et al. [28]) (Fig. 2). These flows were still glassy during our February 2011 observations. Explosive activity observed by the Nov–Dec 2010 group led to formation of a scoria cone that surrounded the former South Pit crater [28], visible as a dark feature in Fig. 2 (obtained commercially for Google Earth in March 2011). At the time of our February 2011 observations, this scoria cone contained a crater and the lava lake, still centered on the previously existing lake location in the South Sink (Fig. 2; see also Field et al. Figs. 1 and 2 [28]).

During our observations, which spanned 1.5 h during the night, we viewed the lava lake from a distance of ~6 m from the rim of the crater containing the lake, which was 39 m × 30 m in diameter. The lake had a thin crust that propagated waves of sub-meter wavelength from fountaining events and contained constantly spreading, incandescent cracks. Fountains and bubble bursts occurred in the lake with a regularity of ~30 s, more frequently for very small bubbles and outgassing events, over an observation time frame of 1.5 h. There were no incandescent jets, as reported by Field et al. [28], though there was minor Strombolian activity associated with the fountaining. There was episodic calving of wall material, or wall spatter, into the lake, which disrupted the crust. See http://youtu.be/XlDJJoFtXIA for a compilation video obtained during this time.

These observations, along with the images and thermal data we obtained, help extend the characterization of eruptive activity at Erta Ale from the end of 2010, described in [28], through early 2011. The final state of activity observed remotely in mid-December 2010 was that of lake level drop to some level below the South Sink crater rim; we observed this level to be steady at 10–15 m below the South Pit crater rim, contained within the scoria cone, during the time of our observations. It is possible the lake rose and fell in the months between Dec and Feb, though the scoria cone and lava overflows appeared to us to be as described by the Nov–Dec 2010 field party, so the lake likely did not overtop the South Pit crater rim in the intervening months.

An image obtained with the Handycam HDR-HC1 camcorder in Normal mode shows the relatively cool lake surface, crater walls and exposed lava fountain (Fig. 4i) from a vantage point ~6 m from the edge of the crater containing the lake, on a 4.5× zoom. We estimate a ground resolution of 0.5 cm–1.0 cm (±1 cm) on the fountain, based on the fact that the largest clots ejected from the fountain, estimated to be ~10 to 30 cm across, are imaged at 20–30 pixels across. The temperature map of the lake region (Fig. 4j) reveals a several hundred degree brightness temperature difference between the lake surface and crater walls and the exposed lava in the fountain and cracks in the lake surface. A rapid decrease in temperature from the centers of the cracks outward is similar to observations of Erta Ale with a thermal imager between 3 and 5 μm [35,25]. Steam emanating from the fountain is illuminated by the exposed lava, leading to overall elevated background temperatures from reflected energy. The bright region in the center of the fountain (Fig. 4j) corresponds with the peak in brightness temperatures obtained by the camcorder of 1164 °C, with some pixels reaching 1176 °C. However, the pixels in this portion of the fountain are at their maximum value, and our observations therefore likely underestimated the lava eruption temperatures. We thus consider this to be a minimum value for the eruption temperature.

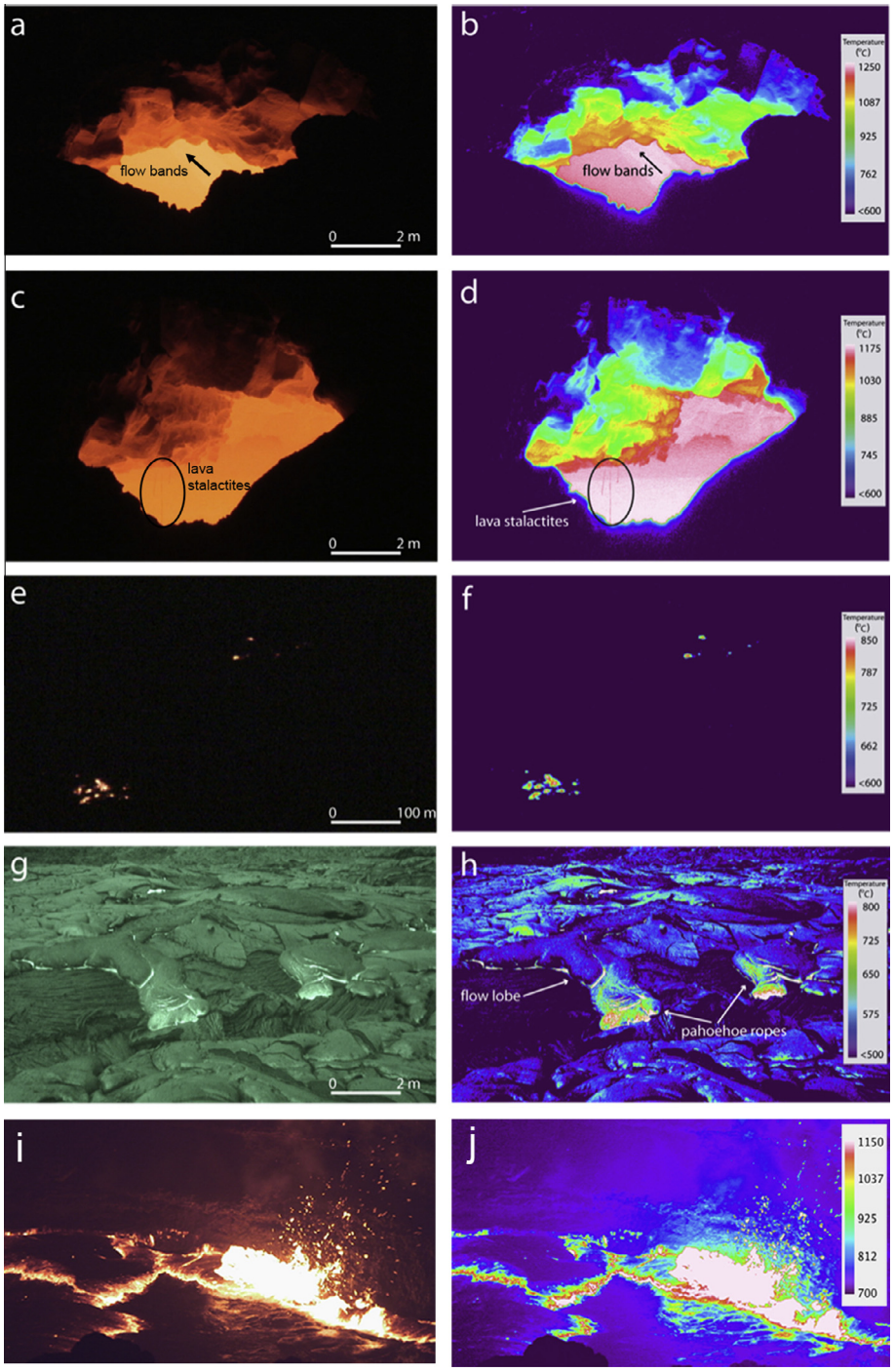

Fig. 4. Digital images (left) and Thermoshot-produced thermal images (right) for the skylight (a–d), surface flow observed from a distance of ~2 km (e–f), and surface flow observed in daylight at ~10 m (g–h). (i) The Erta Ale lava lake in Feb 2011 showing exposed lava in the active fountain and in the cracks on the lake surface. (j) Temperature map of the lava lake. The region shown as white is dominated by brightness temperatures of 1164 °C.

We did not obtain samples for analysis during our observations, and it was not safe or practical to obtain in-situ measurements of the temperatures of the lavas in the lake. However, our values compare favorably with other, recent lava temperature measurements at Erta Ale using in-situ and remote techniques. Burgi et al. [36] measured temperatures at the edges of the Erta Ale lava lake with a thermocouple to be 1187 °C, Oppenheimer and Yirgu [35] found a maximum temperature at a fountain of 1174 °C using a thermal camera at 3–5 μm, Davies et al. [25] found a maximum temperature at a fountain of 1150 °C using a P65 FLIR thermal infrared imager, and Field et al. [28] found temperatures from petrologic analyses of samples to be 1094–1180 °C.

Additionally, at Erta Ale lava lake we explored the potential for low-cost nonimaging detectors to record time variability of lava lake activity. We used a PICAXE 18-X microcontroller to log the output of four detectors collimated by 5 mm aluminum tubes with a view angle of about 5°. These detectors are a CdS photocell (~$1, with response peaking at about 0.5 μm), a Silicon LED (~$1, used as a wavelength-selective photodiode with response at 0.94 μm), an InGaAs photodiode (~$50, response at 1.3 μm) and a thermopile

sensing module using a thermopile detector (~$20, Melexis MLX90601, broadband). In principle, the output of two or more of these detectors could be compared to solve a model for lava lake emission (as has been used for Io) wherein some area fraction of the scene is exposed radiant lava. Unfortunately, because the deployment circumstances prevented a stable tripod mounting, the pointing of the system was not maintained constant (coughing during encounters with SO_2 clouds was a noted perturbation, see http://youtu.be/XlDJJoFtXIA) and a quantitative interpretation of these data has not been attempted. In addition, reported temperatures are significantly lower than eruption temperatures or those obtained by the camcorder. Nonetheless, it is clear (Fig. 5) that all 4 detectors have some time-variable response to a lava lake scene. In constructing a long-term monitor for the variability of lava lake activity (which should be considered 'expendable', with a data acquisition system of the order of $100) a combination of the 0.94 μm and 1.3 μm photodiodes might offer the highest information content.

4. Temperature distributions and fine-scale morphologies

4.1. Temperature distributions

Observations of active volcanism in this study with the Handycam HDR-HC1 reveal high-resolution differences in the areal distribution of brightness temperatures for the skylight, surface flows and lava lake fountains. Brightness temperature maps of the skylight, when "background" is removed, which is all terrain outside the tube interior (and below 600 °C), reveal a narrow distribution of high temperatures (blue curve in Fig. 6).

Similarly, temperatures across the Erta Ale lava lake are consistent with small portions of exposed lavas at cracks and fountains compared with large regions of relatively cool surfaces that insulate hot material beneath. The lava lake fountain and cracks have a narrow distribution of high brightness temperatures, shown as a peak at 1164 °C (yellow curve in Fig. 6), when "background" is removed, which includes the lava lake crust, crater walls, and illuminated steam (temps below 850 °C, red curve in Fig. 6). Brightness temperatures on the lava lake surface peak at ~750 °C, higher than the 500 °C reported by [26], possibly because the camera's dynamic range does not permit simultaneous observations of high and low temperatures. Future observations could include targeted images of lava lake surfaces alone, without hot cracks or fountains, to determine the effect of the dynamic range on the possible spread in temperatures in a single image.

In contrast, the surface flow at Kilauea observed at close range in the daytime displays a wide distribution of brightness temperatures at a lower overall value (green curve in Fig. 6). The broad peak at lower temperatures for this flow reflects the style of eruption in lava flow fields. Very little exposed lava is visible in a surface flow because of rapid heat loss due to convective cooling; however, heat continues to be lost from the interior conductively through a thickening crust [1,3,37], leading to the broad profile of temperatures at relatively lower values.

The distributions of brightness temperatures apparent in Fig. 6 reveal the ability of a lava tube to preserve eruption temperatures at long distances from the vent [e.g., 34, 24], the conductive cooling style at lava flow fields and the insulating ability of lava lake crusts.

4.2. Volcanic feature morphologies

One important value of using the Sony Handycam HDR-HC1 camcorder for observing active eruptions is that it has an image resolution capability (2.8 megapixels) that enables obtaining detailed information on the thermal structure and morphology of lava flows at centimeter to sub-centimeter scale. Flow bands in the lava stream observed in the skylight with the camcorder (Fig. 7a) have fine-scale details observable in the visible images as well as in the thermal images. The highest brightness temperatures in the skylight are observed in the center of the flow, where velocity is highest and the thin crust is disrupted to expose the lava. The camcorder shows that the slower-moving lava adjacent to the margins of the tube is cooler than the central part of the flow, which agrees with data collected by Pinkerton et al. [32].

Lava stalactites can be seen in the skylight with the camcorder (Fig. 7b). Given stalactites are typically <1 cm–3 cm in width, and that ~5 pixels extended across each stalactite, we estimate a resolution of 0.5 cm–1 cm for these features. Several hypotheses exist

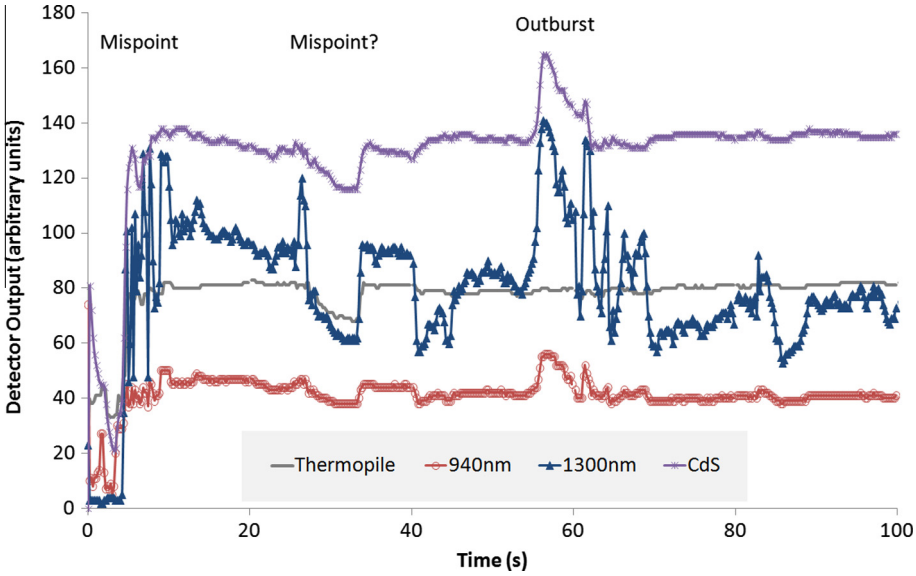

Fig. 5. A time series plot (5 measurements/s) from the Erta Ale observations using four nonimaging detectors. All four detectors show some variations, suggesting their potential utility as low-cost monitors, although the thermopile ('Temp') detector sees little variation since the whole scene is at temperatures above 120 °C – the perturbation at time = 30–35 s is likely due to a mispointing of the system. The InGaAs photodiode with a response at 1300 nm appears to be most sensitive, although the 940 nm Silicon photodiode also shows appreciable fine structure, on time scales that are consistent with appearances of fire fountains.

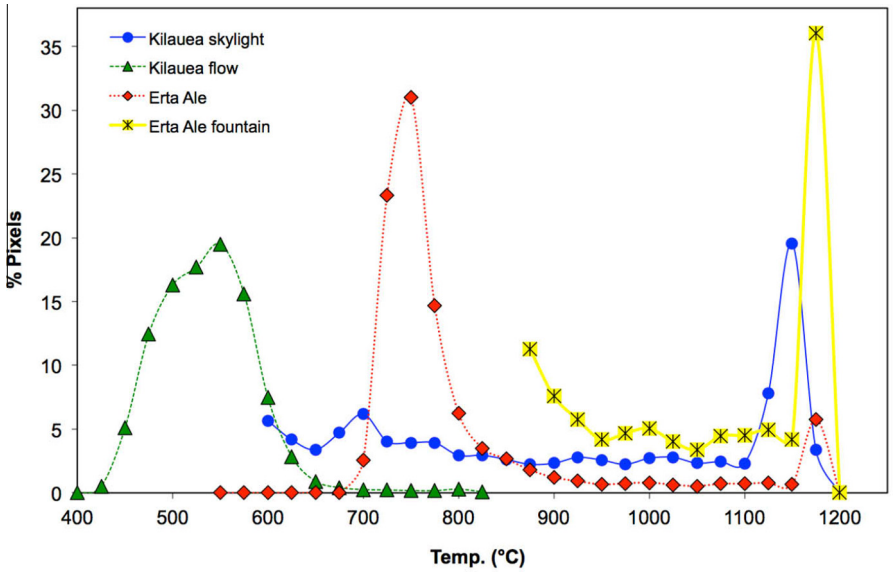

Fig. 6. Distribution of temperatures in each image scene for the Kilauea skylight (blue circles), the Kilauea surface flow (green triangles), the Erta Ale lava lake full scene (red diamonds), and the Erta Ale lava lake fountain and cracks (yellow stars). Peaks in temperature distributions occur near eruption temperatures for the skylight and the lava lake fountain and cracks, while temperatures are distributed more broadly and at lower values for the surface flow and the lava lake surface.

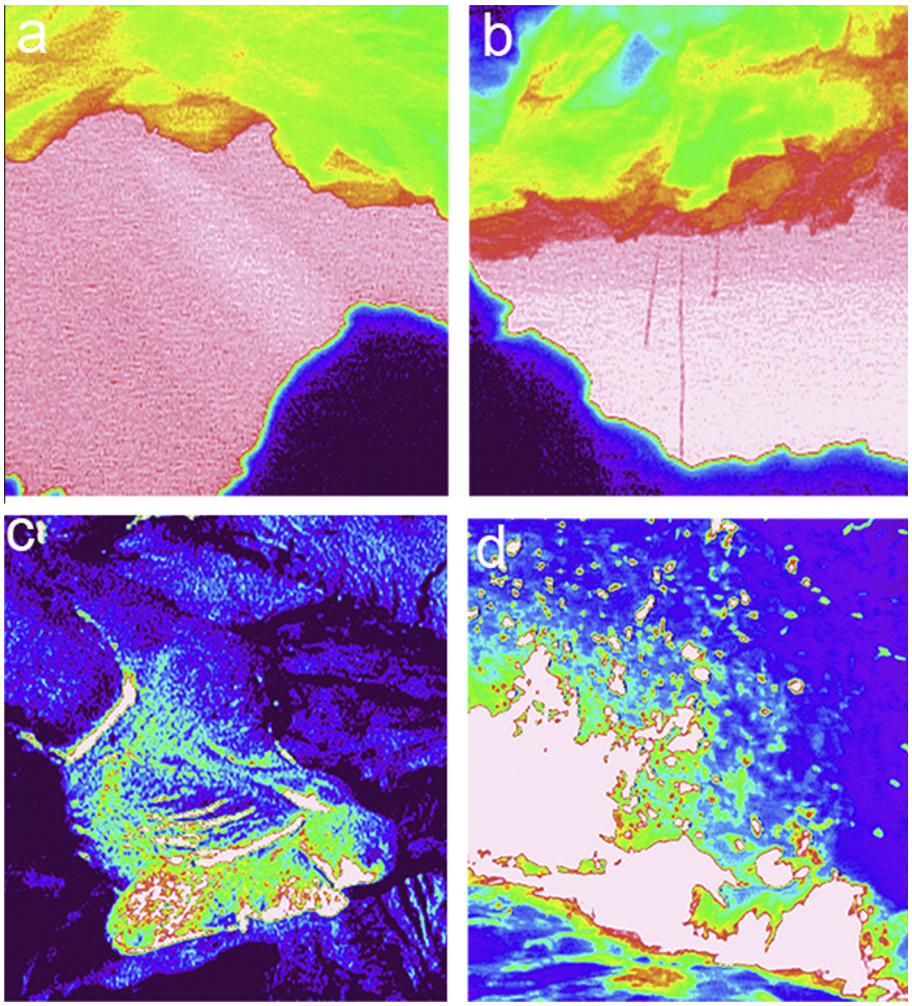

Fig. 7. Details of skylight, lava flow and lava fountain morphologies. (a) Shear thermal textures in the lava flow surface within the skylight. (b) Lava stalactite soda straws on the roof of the lava tube, cooler than the flow surface. (c) Pahoehoe ropes on the flow surface expose hot materials at their fronts. (d) Spatter from the fountain has hot interior and cool rims, cooling more with increasing distance and decreasing size.

to explain the formation of lava stalactites, i.e., dripping of fluid lava from the roof as the tube drains [38] or melting of the tube roof material from temperatures above the solidus [39]. Our data suggest that the stalactites form in close proximity to a hot, active flow, and are at a temperature of ~1000 °C, cooler than the lava flowing in the channel and below the basalt solidus temperature. Though some of the radiation may be a result of reflection from the flow surface, as is likely true for a portion of the walls, these observations are consistent with the formation of stalactites from partially melted roof material, perhaps in which the solidus has been lowered by meteoric water.

The daytime NightShot camcorder images of the surface lava flow clearly reveal the hottest portions of the flow are found below the front edges of the newest lobes. Hot material can be seen underneath a cooler crust (Fig. 7c), providing evidence for inflation [40–43]. Other high brightness temperature regions of the flow can be seen above and behind the forward margin of the flow, indicating the flow is also inflating near the top. Detail can also be seen in the distribution of temperatures across pahoehoe ropes, where temperatures vary several hundred degrees across cooler and newly exposed portions of the ropes, similar to [18] (Fig. 7c). Given the pahoehoe ropes were ~15–25 cm in width, and that ~10 pixels extended across each rope, we estimate the resolution of these images at the pahoehoe ropes to be ~2 cm, ±1 cm.

The lava lake at Erta Ale contains several regions with steep brightness temperature gradients as seen by the camcorder (Fig. 7d). The fountain at the center right of the image is several hundred degrees hotter than the lava lake surface or the crater walls in the background. Ejected blobs of lava are cooler the smaller and more distant they are from the fountain, and the center of the large, 10–30 cm blobs is hotter than the edges, where a thin, cooling crust is being viewed edge-on (Fig. 7d). There is a drop in brightness temperature of several hundred degrees from the center of cracks in the lava lake surface outwards. Typically, the crustal plate on one side of the incandescent crack was spreading away and accreting new material through cooling of exposed lava while the other crustal plate remained relatively stationary, though the whole system slowly migrated across the lake, similar to [26]. The brightness temperature gradient on the spreading plate was several hundred degrees over several tens of centimeters, but on the stationary plate was several hundred degrees over just 1–2 cm. This reveals the powerful insulating character of the lake surface. The fountain itself also seems to follow a path across a crack in the surface, revealing the strength of the lake surface to tearing from fountain activity.

Thermal images of this resolution, sub-centimeter to centimeter, are difficult to obtain with other thermal cameras, especially at such a low cost. These detailed images can be carefully analyzed to determine temperature distributions and eruption morphologies and characteristics. Future applications could include using the system to obtain time series data to model flow and cooling properties of basaltic lavas on centimeter scales.

5. Conclusions

Using low-cost and easily accessible instruments, we observed eruption behaviors, temperatures, morphologies and temperature distributions at low-viscosity, high-temperature eruptions. The short wavelength range and exceptional resolution of the Sony Handycam HDR-HC1 digital camcorder enabled determination of brightness temperatures close to lava eruption temperatures and thermal structure on the scale of sub-centimeter to centimeter. We observed a peak in the maximum brightness temperature at a skylight on Kilauea of 1230 °C and noted a narrow distribution of high brightness temperatures, indicative of lava containment within relatively cool tubes. Observations of surface flows on Kilauea revealed brightness temperatures of 850 °C and centimeter-scale thermal structural differences, such as temperature gradients across ropey pahoehoe. Brightness temperature maps from the surface flow displayed a broad distribution at lower temperatures, a result of the nature of cooling flow surfaces.

Observations of the Erta Ale lava lake obtained just two months after a field campaign by another group extended the baseline of observations for this eruptive episode. We noted that the lava lake that had months earlier filled the crater and overflowed to the caldera margins was now contained within a 39 m × 30 m crater and was fountaining on a ~30 s interval. The peak in maximum brightness temperatures obtained by the camcorder in a lava fountain was at 1164 °C, and though the pixels were at their maximum value, the corresponding temperatures compared well with previous in-situ measurements (1187 °C), petrologic analyses (1180 °C) and thermal camera observations (1174 °C and 1150 °C). The lava lake surface was cooler than the fountain or cracks by several hundred degrees as observed by the camcorder, and temperature gradients across the fountain and cracks were observed on centimeter to sub-centimeter scales. A non-imaging thermal system revealed variations in thermal output that could correspond with the fountaining timescale, especially at 1.3 μm.

Detailed analyses of morphologies and temperatures on a range of scales and over time using these portable systems can lead to an increased understanding of volcano structure and behavior, lava rheology, cooling behavior, and response to stress. Using a time-series approach, these systems could also detect changes in an eruption magnitude or location or analyze rates of cooling over time.

Similar characteristics for an imaging system – high spatial resolution, rapid image acquisition, and the ability to obtain eruption temperatures – are necessary attributes for imaging active volcanoes on Jupiter's moon Io [44,25]. Volcanoes are constantly erupting across the body in lava flows, tubes, and fountaining lava lakes [45,46,30,47]. Lavas there are mafic to ultramafic silicate in composition, so they require imaging in the same spectral range as the Handycam – visible to short-wavelength infrared – in order to obtain accurate eruption temperatures at appropriate image resolutions (with the addition of multi-color data; [44,25]). Such instruments are under consideration for future Io missions [48]. Continued studies of volcanoes on Earth using these accessible systems, in conjunction with field studies and other thermal imaging systems, can lead to a better understanding of volcanic eruption behaviors as observed through remote sensing, which will enable better interpretations of observations of volcanoes on Io.

Acknowledgments

We would like to thank the Hawaii Volcanoes Observatory and 13 Suns Tours, Addis Ababa for help and cooperation in collecting data on the active flow field and the lava lake. We thank two anonymous reviewers for their valuable input to revisions of this manuscript. We thank Brigham Young University's College of Physical and Mathematical Sciences and Department of Geological Sciences for funding and field support. Part of this work was carried out at the Jet Propulsion Laboratory, California Institute of Technology, under contract with NASA.

References

[1] Flynn LP, Mouginis-Mark PJ. Cooling rate of an active Hawaiian lava flow from nighttime spectroradiometer measurements. Geophys Res Lett 1992;19:1783–6.
[2] Flynn LP, Mouginis-Mark PJ. Temperature of an active lava channel from spectral measurements, Kilauea Volcano Hawaii. Bull Volcanol 1994;56:297–301.

[3] Harris AJL, Dehn J, James MR, Hamilton C, Herd R, Lodato L, et al. Pahoehoe flow cooling, discharge, and coverage rates from thermal image chronometry. Geophys Res Lett 2007;34:L19303.
[4] Harris AJL. Thermal remote sensing of active volcanoes: a users manual. West Nyack, NY: Cambridge University Press; 2013. 756 pp.
[5] Spampinato L, Calvari S, Oppenheimer C, Boschi E. Volcano surveillance using infrared cameras. Earth-Sci Rev 2011;106:63–91.
[6] Oppenheimer C, Francis PW, Rothery DA, Carlton RWT. Infrared image analysis of volcanic thermal features – Lascar Volcano, Chile, 1984–1992. J Geophys Res 1993;98:4269–86.
[7] Dehn J, Dean K, Engle K. Thermal monitoring of North Pacific volcanoes from space. Geology 2000;28:755–8.
[8] Davies AG, Keszthelyi LP, Williams DA, Phillips CB, McEwen AS, Lopes RMC, et al. Thermal signature, eruption style, and eruption evolution at Pele and Pillan on Io. J Geophys Res Planets 2001;106:33079–103.
[9] Harris AJL, Rowland SK. FLOWGO: a kinematic thermo-rheological model for lava flowing in a channel. Bull Volcanol 2001;63:20–44.
[10] Pieri D, Abrams M. ASTER observations of thermal precursors to the April 2003 eruption of Chikurachki Volcano, Kurile Islands, Russia. Remote Sens Environ 2005;99:84–94.
[11] Vaughan RG, Hook SJ, Ramsey MS, Realmuto VJ, Schneider DJ. Monitoring eruptive activity at mount St. Helens with TIR image data. Geophys Res Lett 2005;32:L19305.
[12] Davies AG, Chien S, Baker V, et al. Monitoring active volcanism with the Autonomous Sciencecraft Experiment on EO-1. Remote Sens Environ 2006;101:427–46.
[13] McEwen AS, Belton MJS, Breneman HH, Fagents SA, Geissler P, Greeley R, et al. Galileo at Io: results from high-resolution imaging. Science 2000;288:1193–8.
[14] Marchis F, Le Mignant D, Chaffee FH, et al. Keck AO survey of Io global volcanic activity between 2 and 5 microns. Icarus 2005;176:96–122.
[15] Spencer JR, Stern SA, Cheng AF, Weaver HA, Reuter DC, Retherford K, et al. Io volcanism seen by New Horizons; a major eruption of the Tvashtar Volcano. Science 2007;318:240–3.
[16] Ramsey MS, Harris AJL. Volcanology 2020: how will thermal remote sensing of volcanic surface activity evolve over the next decade? J Volcanol Geoth Res 2013;249:217–33.
[17] Wright R, Flynn LP. On the retrieval of lava flow surface temperatures from infrared satellite data. Geology 2003;31:893–6.
[18] Calvari S, Spampinato L, Lodato L, Harris AJL, Patrick MR, Dehn J, et al. Chronology and complex volcanic processes during the 2002–2003 flank eruption at Stromboli (Italy) reconstructed from direct observation and surveys with a handheld thermal camera. J Geophys Res 2005;110:B02201.
[19] Harris AJL, Dehn J, Patrick M, Calvari S, Ripepe M, Lodato L. Lava effusion rates from hand-held thermal infrared imagery: an example from the June 2003 effusive activity at Stromboli. Bull Volcanol 2005;68:107–17.
[20] Ando B, Pecora E. An advanced video-based system for monitoring active volcanoes. Comput Geosci 2006;32:85–91.
[21] James MR, Robson S, Pinkerton H, Ball M. Oblique photogrammetry with visible and thermal images of active lava flows. Bull Volcanol 2006;69:105–8.
[22] Carter AJ, Ramsey MS, Belousov AB. Detection of a new summit crater on Bezymianny Volcano lava dome: satellite and field-based thermal data. Bull Volcanol 2007;69:811–5.
[23] Coppola D, Staudacher T, Cigolini C. Field thermal monitoring during the August 2003 eruption at Piton de la Fournaise (La Reunion). J Geophys Res 2007;112:B05215.
[24] Witter JB, Harris AJL. Field measurements of heat loss from skylights and lava tube systems. J Geophys Res 2007;112:B012303.
[25] Davies AG, Keszthelyi L, McEwen AS. Estimating eruption temperature from thermal emission spectra of lava fountain activity in the Erta'Ale (Ethiopia) volcano lava lake: implications for observing Io's volcanoes. Geophys Res Lett 2011;38. http://dx.doi.org/10.1029/2011GL049418.
[26] Spampinato L, Oppenheimer C, Calvari S, Cannata A, Montalto P. Lava lake surface characterization by thermal imaging: Erta 'Ale volcano (Ethiopia). Geochem Geophys Geosyst 2008;9:Q12008. http://dx.doi.org/10.1029/2008GC002164.
[27] Saito T, Sakai S, Iizawa I, Suda E, Umetani K, Kaneko K, et al. A new technique of radiation thermometry using a consumer digital camcorder: observations of red glow at Aso Volcano, Japan. Earth Planets Space 2005;57:e5–8.
[28] Field L, Barnie T, Blundy J, Brooker RA, Keir D, Lewi E, et al. Integrated field, satellite and petrological observations of the November 2010 eruption of Erta Ale. Bull Volcanol 2012;74:2251–71.
[29] Ball M, Pinkerton H. Factors affecting the accuracy of thermal imaging cameras in volcanology. J Geophys Res 2006;111:B11203.
[30] Radebaugh J, McEwen AS, Milazzo MP, Keszthelyi LP, Davies AG, Turtle EP, et al. Observations and temperatures of Io's Pele Patera from *Cassini* and *Galileo* spacecraft images. Icarus 2004;169:65–79.
[31] Swanson DA. Pahoehoe flows from the 1969–1971 Mauna Ulu eruption, Kilauea volcano, Hawaii. GSA Bull 1973;84:615–26.
[32] Pinkerton H, James M, Jones A. Surface temperature measurements of active lava flows on Kilauea volcano, Hawaii. J Volcanol Geoth Res 2002;113:159–76.
[33] Rothery DA, Francis PW, Wood CA. Volcano monitoring using short wavelength infrared data from satellites. J Geophys Res 1988;93:7993–8008.
[34] Keszthelyi L. A preliminary thermal budget for lava tubes on the earth and planets. J Geophys Res 1995;100:20411–20.
[35] Oppenheimer C, Yirgu G. Thermal imaging of an active lava lake: Erta'Ale volcano, Ethiopia. Int J Remote Sens 2002;22:4777–82.
[36] Burgi P-Y, Caillet M, Haefeli S. Field temperature measurements at Erta'Ale Lava Lake, Ethiopia. Bull Volcanol 2002;64:472–85.
[37] Keszthelyi L, Denlinger R. The initial cooling of pahoehoe flow lobes. Bull Volcanol 1996;58:5–18.
[38] Corsaro RA, Calvari S, Pompilio M. Formation of lava stalactites in the master tube of the 1792–1793 flow field, Mt. Etna (Italy). Am Mineral 2005;90:1413–21.
[39] Kauahikaua J, Cashman KV, Mattox TN, Heliker CC, Hon KA, Mangan MT, et al. Observations on basaltic lava streams in tubes from Kilauea Volcano, island of Hawaii. J Geophys Res Solid Earth 1998;103:27303–23.
[40] Hon K, Kauahikaua J, Denlinger R, Mackay K. Emplacement and inflation of pahoehoe sheet flows; observations and measurements of active lava flows on Kilauea Volcano, Hawaii. GSA Bull 1994;106:351–70.
[41] Self S, Thordarson T, Keszthelyi L, Walker GPL, Hon K, Murphy MT, et al. A new model for the emplacement of Columbia River basalts as large, inflated pahoehoe lava flow fields. Geophys Res Lett 1996;23:2689–92.
[42] Calvari S, Pinkerton H. Lava tube morphology on Etna and evidence for lava flow emplacement mechanisms. J Volcanol Geophys Res 1999;90:263–80.
[43] Burkhard DJ. Thermal interaction between lava lobes. Bull Volcanol 2003;65:136–43.
[44] McEwen AS, Keszthelyi L, Spencer JR, Schubert G, Matson DL, Lopes-Gautier R, et al. High-temperature silicate volcanism on Jupiter's moon Io. Science 1998;281:87–90.
[45] Lopes-Gautier R, McEwen AS, Smythe WB, Geissler PE, Kamp L, Davies AG, et al. Active volcanism on Io: global distribution and variations in activity. Icarus 1999;140:243–64.
[46] Davies AG. Volcanism on Io: a comparison with earth. Cambridge, UK: Cambridge University Press; 2007. 355 pp.
[47] Allen DA, Radebaugh J, Stephens D. Temperature and variability of Pillan, Wayland Patera, and Loki Patera on Io from Cassini ISS data. Icarus 2013;226:77–88.
[48] McEwen AS, Turtle E, Hibbard K, Reynolds E, Adams E. Io volcano observer (IVO): budget travel to the outer solar system. Acta Astronaut 2014;93:539–44.